Neuropsychologia 49 (2011) 1177–1186

Contents lists available at ScienceDirect

Neuropsychologia

journal homepage: www.elsevier.com/locate/neuropsychologia

A dynamic causal modeling analysis of the effective connectivities underlying top-down letter processing

Jiangang Liu[a], Jun Li[b], Cory A. Rieth[d], David E. Huber[d], Jie Tian[b,c,*], Kang Lee[d,e,**]

[a] Department of Biomedical Engineering, School of Computer and Information Technology, Beijing Jiaotong University, Beijing 100044, China
[b] School of Life Sciences and Technology, Xidian University, Xi'an 710071, China
[c] Institute of Automation, Chinese Academy of Sciences, P.O. Box 2728, Beijing 100190, China
[d] University of California, San Diego, CA, USA
[e] University of Toronto, Canada

ARTICLE INFO

Article history:
Received 2 September 2010
Received in revised form 9 December 2010
Accepted 6 January 2011
Available online 13 January 2011

Keywords:
Letter processing
Word processing
Top-down processing
fMRI
Dynamic causal modeling

ABSTRACT

The present study employed dynamic causal modeling to investigate the effective functional connectivity between regions of the neural network involved in top-down letter processing. We used an illusory letter detection paradigm in which participants detected letters while viewing pure noise images. When participants detected letters, the response of the right middle occipital gyrus (MOG) in the visual cortex was enhanced by increased feed-backward connectivity from the left inferior frontal gyrus (IFG). In addition, illusory letter detection increased feed-forward connectivity from the right MOG to the left inferior parietal lobules. Originating in the left IFG, this top-down letter processing network may facilitate the detection of letters by activating letter processing areas within the visual cortex. This activation in turns may highlight the visual features of letters and send letter information to activate the associated phonological representations in the identified parietal region.

© 2011 Elsevier Ltd. All rights reserved.

1. Introduction

Reading is a fundamental skill for individuals living in any modern society. Difficulty in reading can have debilitating social and cognitive consequences. Although there is evidence of holistic word processing during reading (for a review, see Cohen & Dehaene, 2004), identification of each separate letter is necessary to read a word (Pelli, Farell, & Moore, 2003). Recent studies of the neural mechanisms supporting reading have identified a hierarchical cortical model of visual word processing (Dehaene, Cohen, Sigman, & Vinckier, 2005; Vinckier et al., 2007). This word processing network starts in the primary visual cortex, which processes the separate line segments forming each letter. Higher areas within the visual cortex process the letters in an increasingly abstract manner. Ultimately, information is projected to the left middle fusiform gyrus, specifically a region termed the 'visual word form area' (VWFA), where letters are integrated to identify specific combinations of letters (i.e., letter strings) independent of location, size, and case (Cohen & Dehaene, 2004; McCandliss, Cohen, & Dehaene, 2003; but see Price & Devlin, 2003; Reinke, Fernandes, Schwindt, O'Craven, & Grady, 2008 for other interpretations of this area). Demonstrating the importance of this area, deafferentation of the VWFA from the visual cortex input is associated with reading impairments (Cohen et al., 2003).

Beyond this network that projects to the VWFA, recent studies have also revealed a network involving the visual, parietal and prefrontal regions specific to letter processing. For example, Flowers et al. (2004) demonstrated that the left middle occipital gyrus (MOG) and bilateral inferior frontal gyrus (IFG) were activated by a single letter as compared to a symbol or a color. More recently, James and Gauthier (2006) revealed that the left fusiform gyrus and the left IFG showed a greater response to letters than to that of objects and faces. Finally, Joseph, Gathers, and Piper (2003) found letter-selective activation as compared to objects and noise images within the left inferior parietal regions and the left insula. However, these studies can only specify the nature of this network in terms of bottom-up, or stimulus driven, letter processing because they used clearly visible high contrast letters.

Despite this focus on bottom-up processing with neuroimaging studies, behavioral studies have consistently demonstrated an important role for top-down expectations in letter and word processing (Nazir, Jacobs, & O'Regan, 1998; Reicher, 1969). Little is, however, known about the neural networks involved in top-down

* Corresponding author at: Institute of Automation, Chinese Academy of Sciences, P.O. Box 2728, Beijing 100190, China. Tel.: +86 10 82618465; fax: +86 10 62527995.
** Corresponding author at: University of Toronto, Canada.
E-mail addresses: tian@ieee.org (J. Tian), kang.lee@utoronto.ca (K. Lee).

0028-3932/$ – see front matter © 2011 Elsevier Ltd. All rights reserved.
doi:10.1016/j.neuropsychologia.2011.01.011

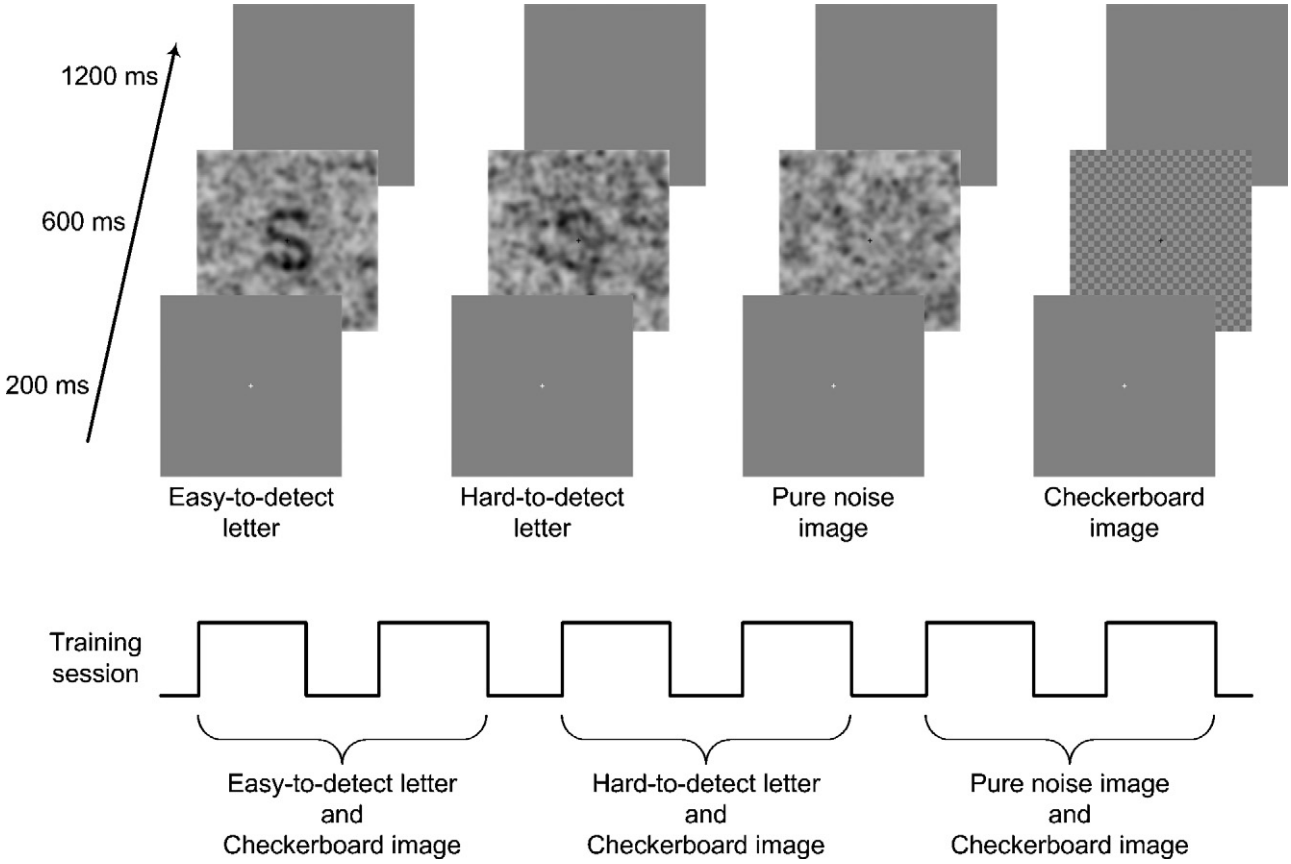

Fig. 1. Examples of stimuli and illustration of experimental paradigm.

processing of letters and only a handful neuroimaging studies have examined top-down letter processing. For instance, Kosslyn et al. (1993) found more activation within the bilateral dorsolateral prefrontal cortex for imagery of a letter as compared to perception of a letter. James and Gauthier (2006) found that imagining letters induced a greater response in the left IFG relative to drawing letters. Stokes, Thompson, Cusack, and Duncan (2009) found that the bilateral lateral occipital complex (LOC) was activated by both perception and imagination of specific letters.

Recently, Liu et al. (2010) used an illusory detection paradigm to identify the network involved in top-down letter processing. In their study participants were presented with noisy images and instructed to indicate whether a letter was present. In fact, after an initial training period of increasing detection difficulty, the images contained only noise. This method of studying top-down influences by eliciting illusory detection has advantages over both pure mental imagery paradigms that present no stimulus, and paradigms where a letter is actually presented. Although activations during mental imagery are purely top-down, they may not activate the areas involved in the visual perception of letters, and thus have difficulty to specify the role that these visual perception areas may play in top-down letter processing. In contrast, presentation of actual letters will activate the visual perception areas, but may fail to strongly evoke the top-down network. Illusory perception strikes a balance by providing some visual input, which activates low-level visual areas, while highlighting the role of top-down expectations during perception because the visual input does not strongly indicate a particular perception. Using this pure noise illusory letter detection paradigm, Liu et al. (2010) found that the left IFG, the left superior parietal lobule (SPL), and the right MOG were more active when participants falsely detected a letter while viewing a pure noise image (the letter response) as compared to trials where they did not detect a letter (the no-letter response). Thus, these brain regions appear to be involved in the top-down processing of letters.

Because Liu et al. (2010) used a conventional BOLD analyses, it is unclear how these top-down letter processing regions are functionally connected during top-down letter processing. Previous studies found that the response of category-preferential regions within the visual cortex can be modulated by feed-backward connections from the frontal cortex (Mechelli, Price, Friston, & Ishai, 2004; Summerfield et al., 2006). In the current study, we hypothesized that a top-down projection from the identified anterior brain areas (e.g., the left IFG) may exert feedback on the right MOG. Our hypothesis was based on the existing findings regarding top-down letter processing. By examining letter naming (Joseph, Cerullo, Farley, Steinmetz, & Mier, 2006), letter imagining (James & Gauthier, 2006) and illusory letter detection (Liu et al., 2010), the left IFG's involvement in top-down letter processing has been identified. However, no prior neural imaging studies have identified whether this involvement of the left IFG occurs through feed-backward connections. The present study was thus conducted to test this hypothesis specifically.

To ascertain the existence of this hypothesized top-down connection, the present study used the same pure noise image paradigm as Liu et al. (2010). In addition, to identify the effective connections among the neural regions involved in top-down letter processing, we used dynamic causal modeling (DCM, Friston, Harrison, & Penny, 2003). DCM treats the brain as an input-state-output system, and uses the known input design and the time course of measured responses in each brain region to estimate various parameters that characterize the interaction between brain regions. This method allowed us to identify feed-backward and feed-forward connections among the regions of the neural net-

work recruited when participants detected letters in pure noise images.

2. Methods

2.1. Participants

Eighteen healthy, right-handed Chinese adults (8 males, age: 18–28) with normal or corrected-to-normal vision participated in the present study after giving their informed consent. All participants had at least ten-year's experience reading Roman letters since at least Grade 1. This study was approved by the Human Research Protection Program of Tiantan Hospital, Beijing, China.

2.2. Stimuli and procedure

Three types of stimuli were used: pure-noise images, ease-to-detect letters, and hard-to-detect letters. Easy-to-detect letters and hard-to-detect letters were produced by subtracting a blurred version of a letter (a, s, c, e, m, n, o, r, or u) from the pure-noise image at 60% and 35% of its full value, respectively (for more details see Liu et al., 2010). Checkerboard-images were used as the baseline stimulus. Fig. 1 shows an example for each stimulus type.

The experiment included an initial training period, a testing period, and a functional localizer period. Participants were scanned only during the testing period and the functional localizer period. As shown in Fig. 1, the training session consisted of six 56-s letter-detection blocks, each of which included randomly presented 20 task images and 8 checkerboard images. The first two blocks contained an equal number of easy-to-detect letters and pure-noise images. The next two blocks contained an equal number of hard-to-detect letters and pure-noise images. In the last two blocks of the training period, all images were pure noise images. Participants were told that in each block, half of the 20 task images contained letters, and half did not. They were instructed to press a button on a response device with their left or right index finger (counterbalanced across participants) if they detected a letter in the task image. Alternatively, if they decided that the image did not contain a letter, they were to press a button with their index finger of the opposite hand. No responses were required to the checkerboard images. Both the task images and checkerboards were presented for 600 ms after a 200-ms fixation crosshair. Following each task image, a blank screen appeared for 1200 ms. The training session was designed to teach participants the nature of the experiment, and to keep them on task at detecting letters even when viewing pure noise images.

Following training, there were four testing sessions, each of which contained 40 checkerboard images and 120 pure-noise task images presented in random order. The procedure for these test trials was the same as the last two blocks of the training. The test trials only contained pure-noise images although participants were told that half of the images contained letters and the other half did not.

To identify brain areas responsive to real letters, two functional localizer sessions were performed after the letter detection task. Both localizer sessions included two 20-s real letter or noise image epochs with 14-s intervals of fixation between epochs. During the localizer sessions, participants monitored the images and pressed a response key whenever an intermittent white square appeared at the edge of the picture (this procedure ensured that participants were paying attention during the passive viewing task).

2.3. Functional MRI data acquisition

Structural and functional MRI data were collected using a 3.0 T MR imaging system (Siemens Trio, Germany) at Tiantan Hospital. Whole brain fMRI volumes were acquired using a single shot, T2*-weighted gradient-echo planar imaging (EPI) sequence (interleaved orders, TR/TE = 2000/30 ms; FOV = 240 mm; matrix = 64 × 64; 32 slices; 4 mm thickness). High-resolution structural images were acquired using a three-dimensional enhanced fast gradient-echo sequence (FOV = 256 mm, matrix = 256 × 256; 256 slices; 1 mm thickness).

2.4. Statistical parametric mapping analysis

Image analysis included preprocessing and statistical analyses, which were performed using the Statistical Parametric Mapping software (SPM5, Wellcome Department of Imaging Neuroscience, London, UK; http://www.fil.ion.ucl.ac.uk/spm Friston et al., 1995). After slice-timing correction (reference slice = 31) and spatial realignment and normalization to the MNI152 template (Montreal Neurological Institute), all testing session scans were resampled into $2 \times 2 \times 2\,mm^3$ voxels, and then spatially smoothed with an isotropic 6 mm full-width-half-maximal (FWHM) Gaussian kernel to decrease spatial high frequency noise and ensure the validity of inferences based on parametric tests.

For each participant, the four testing sessions were concatenated into one single session with an additional four regressors to account for sessions effects (Bitan et al., 2005). This one session was high-pass filtered (high-pass filter = 128 s) to remove low frequency noise such as scanner drift (Friston et al., 1995). Trials were classified according to whether participants produced the letter response or the no-letter response. A General Linear Model (GLM) applied to the data included three regressors corresponding to letter responses, no-letter responses, and pure-noise images regardless of the chosen response. Each regressor was created by convolving a canonical hemodynamic response function (HRF) with a delta function corresponding to the presentation sequence of each stimulus category. Movement parameters were used in the GLM as regressors to account for residual effects related to movement.

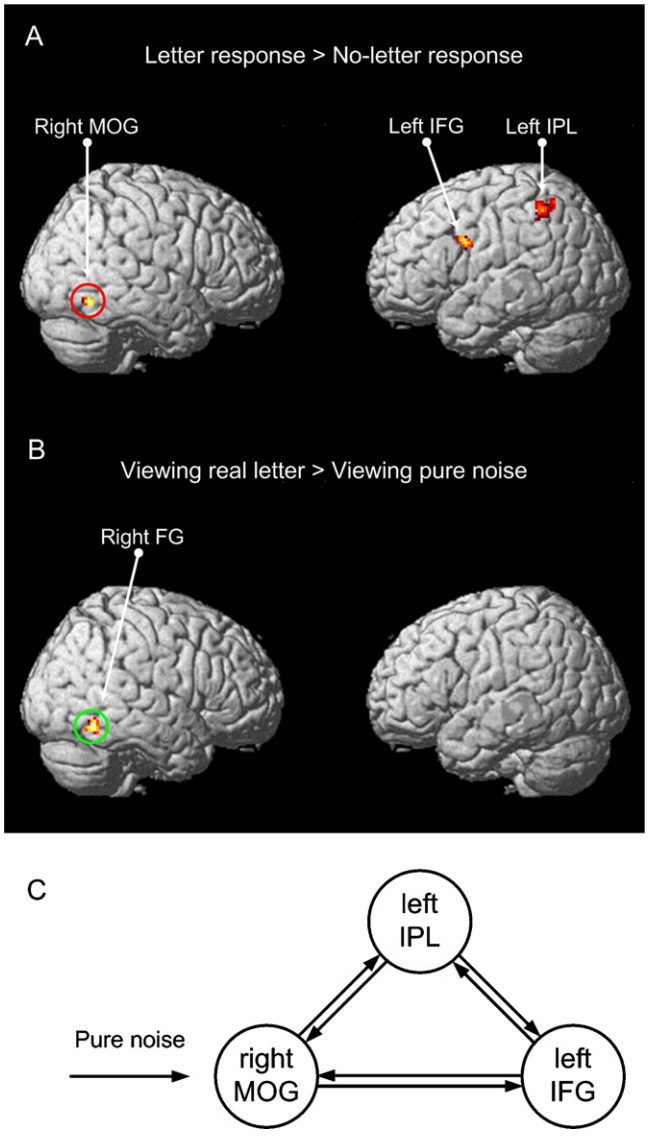

Fig. 2. (A) The group results comparing the letter responses to the no-letter responses during the experimental test sessions ($p < 0.007$ FDR corrected, $k > 30$); (B) the group results comparing the viewing of real letters to the viewing of pure noise images during the functional localizer session ($p < 0.007$ FDR corrected, $k > 30$); and (C) the basic model with full reciprocal intrinsic connections. The input was assumed to drive the right MOG directly. MOG, the middle occipital gyrus; IPL, the inferior parietal lobules; IFG, the inferior frontal gyrus; FG, the fusiform gyrus.

With respect to the localizer sessions, the fMRI data for each participant were processed using the same steps as those used for the testing sessions, except that two regressors were created for viewing real letters versus viewing pure noise images.

Participant-specific contrast images were calculated using a whole brain analysis. One of these contrast images compared letter responses and no-letter responses for the testing sessions and the other compared real letters and pure noise images for the localizer sessions. Group results were obtained using random effects analysis by averaging participant-specific contrast images across all participants, as tested with a statistical threshold of $p < 0.007$ (FDR corrected for multiple comparisons) and cluster threshold of $k > 30$.

2.5. DCM analysis

Using the DCM, three sets of parameters can be estimated: the extrinsic influence of inputs on regional responses, the intrinsic connections between regions that reflect the interregional impact in the absence of experimental manipulations, and

Table 1
Group activation results comparing letter responses versus no-letter response and comparing passive viewing of letters versus pure noise images ($p < 0.007$ FDR corrected, $k > 30$).

Brain regions	Hemisphere	Cluster voxels	MNI coordinates			Z
			x	y	z	
Letter response minus no-letter response						
Inferior frontal gyrus	Left	73	−52	6	30	4.57
Inferior parietal lobules	Left	195	−40	−48	52	4.87
Middle occipital gyrus	Right	44	52	−60	−12	4.85
No-letter response minus letter response						
No results						
Viewing real letters versus viewing pure noise						
Fusiform gyrus	Right	81	48	−56	−10	5.10

the modulatory effect that reflects the change in intrinsic connections induced by the processing of specific experimental stimuli (Friston et al., 2003; Mechelli et al., 2004). Given the purpose of the present study, we were most interested in the modulatory effect for letter responses. As adopted by Stephan, Marshall, Penny, Friston, and Fink (2007) and Chow, Kaup, Raabe, and Greenlee (2008), a two-level procedure was used for the DCM analysis in the present study. In the first-level, candidate models were produced for each participant and the best model was selected using Bayesian model selection. All these analyses were implemented with the DCM tool in SPM5 (Friston et al., 2003; Penny, Stephan, Mechelli, & Friston, 2004).

2.5.1. Region selection and time series extraction

Regions showing more activation during the experimental testing sessions for letter responses than for no-letter responses were used to define volumes of interest (VOIs), which were included in the DCM models. As revealed in the group results, more activation for letter responses than no-letter responses was observed in the left inferior frontal gyrus (IFG), the left inferior frontal lobules (IPL) and the right middle occipital gyrus (MOG) (Fig. 2A and Table 1).

Participant-specific VOIs were selected based on conventional SPM group results. To allow for individual differences in the peak activation locations, each participant's t-contrast map was used to identify a participant-specific maximum, which was the nearest local maximum within 15 mm of the local maximum of the group analysis. Based on these maxima, regional responses were defined as the first principal component of the time series from all voxels included in a 6-mm-radius spherical volume centered at each participant's maximum. It should be noted that the present study used the same data (i.e., the testing sessions) for the definition of VOIs in conventional fMRI analyses and the time series extractions in the DCM analysis. However, the conventional analysis and the DCM analysis aimed to address generally different issues, and thus there was not circularity in the analysis (see Stephan et al., 2010). Using these procedures, 3 VOIs were identified for each of 17 participants: the left IFG (MNI: -51 ± 5, 7 ± 4, 30 ± 5), the left IPL (MNI: -38 ± 4, -46 ± 6, 50 ± 6), and the right MOG (MNI: 49 ± 3, -59 ± 5, -12 ± 4), and Table 2 lists the loci of VOIs for each participant. One participant was not included in the DCM analysis because that participant did not produce 3 VOIs meeting all the criteria for VOI selection.

2.5.2. Definition of anatomical connection and driving input

A basic model was constructed with reciprocal intrinsic connections between the VOIs (Fig. 2C). The regressor encoding the pure-noise images was defined as the driving input. This input was assumed to drive the right MOG (Fig. 2A, red circle) because the right MOG is located in the visual cortex (i.e., among these 3 VOIs, the right MOG is likely the locale to receive information from the lower visual areas) and because the location of the right MOG was highly consistent with (1) the region responding more to passively viewed letters than passively viewed noise images (Fig. 2B, green circle), (2) prior knowledge from the existing neuroimaging studies (Dehaene et al., 2005), and (3) neuropsychological studies (Cohen et al., 2003). Thus, the activation to a pure noise image was assumed to be propagated from the right MOG to other regions (i.e., the left IPL and the left IFG) by the assumed intrinsic connection between the VOIs.

2.5.3. Definition of modulatory inputs

With the assumed basic model, we examined how the intrinsic connections changed as a function of illusory letter detection. We were most interested in whether there were enhanced feed-backward connections from the high-order cortical regions (i.e., the left IPL or the left IFG) to the visual cortex (i.e., the right MOG) when a letter was detected while viewing a pure noise image. Therefore, the regressor that encoded the letter responses was used as a modulatory input specified on the intrinsic connections between two VOIs of the basic model. Additionally, because the above GLM results suggest that all three VOIs were co-activated during the letter versus no-letter responses, we assumed that all modulatory models must satisfy the criterion whereby each VOI must modulate at least another VOI. Further, because we had no a priori knowledge about the directions of the interactions between the VOIs, we tested all possible directions of interaction for each connection: feed-forward, feed-backward, or reciprocal. With these considerations, an exhaustive set of 54 possible modulatory models was generated by specifying the modulatory effect of letter responses on different combinations of intrinsic connections of the basic model (Fig. 3, M1–M54).

However, these models only included the modulatory effects of the letter response but not that of the no-letter responses. Thus, even when the intrinsic connections of these models might be enhanced during the letter response trials, one may not be able to attribute such modulatory effects to the letter responses *per se*. This is because these enhanced effects could be due to the shared effects of the letter responses and the no-letter responses. In other words, the letter detection task demand itself, not just the illusory detection of non-existent letters, might engender the modulatory effects. To address this issue, another set of 54 possible models was generated. Unlike the above 54 possible models, the new set of 54 possible models specified both the modulatory effects of the letter responses and those of the no-letter responses (Fig. 4, M55–M108). As a result, there were 108 candidate models in total in the present DCM analysis, between which Bayesian model selection (BMS) was performed.

2.5.4. Bayesian model selection

For each participant, after all candidate models were estimated, they were compared in a pairwise fashion using Bayesian model selection (BMS) to determine which DCM model was the best (Penny et al., 2004). To compare model m_i and m_j, the Bayes factor (BF) was calculated based on the Bayesian information criterion (BIC) as well as the Akaike information criterion (AIC) using the equation:

$$\mathrm{BF}_{ij} = \frac{p(y|m_i)}{p(y|m_j)}$$

If the BFs based on both BIC and AIC are $\geq e$, there is said to be consistent evidence for the superiority of m_i over m_j (Penny et al., 2004). At the group level, the comparison among models was usually based on the group Bayes factor (GBF), which was defined as the product of all individual BFs. However, because the GBF is susceptible to outliers, we additionally used the 'Positive Evidence Ratio' (PER) as a supplemental measure in the selection of the best model (Raftery, 1995; Stephan & Penny, 2006). This more conservative measure stipulates that model i is superior to j only for $\mathrm{BF} > 3$. It should be noted that the GBF index corresponds to a fixed effects (FFX) analysis whereby it assumes all participants have the same optimal model (see Stephan, Penny, Daunizeau, Moran, & Friston, 2009; Stephan et al., 2010 for discussion of potential limitations of this procedure).

2.5.5. Second-level analysis of model parameters

After model selection, a one-sample t-test was performed separately for each parameter of the intrinsic connections and modulatory effects for the best model. The aim of these tests was to examine whether the parameters were larger than zero in general, across all 17 participants. A conservative statistical threshold of $p < 0.05$ with Bonferroni's correction was adopted for the one-sample tests.

3. Results

3.1. Statistical parametric mapping results

Participants detected letters on 37.7% (SD: 20.0%) of the 480 pure noise detection trials. There was no significant difference in response time between letter responses and no-letter responses (letter response: Mean = 789.05 ms, SD = 197.54 ms; no-letter response: Mean = 774.79 ms, SD = 180.15 ms; $t(17) = 0.752$, $p = 0.462$).

As shown in Fig. 2A, for the experimental testing sessions, regions showing more activation for letter response trials than for no-letter response trials were identified within the left IFG, the left IPL, and the right MOG with a significant threshold of $p < 0.007$ (FDR

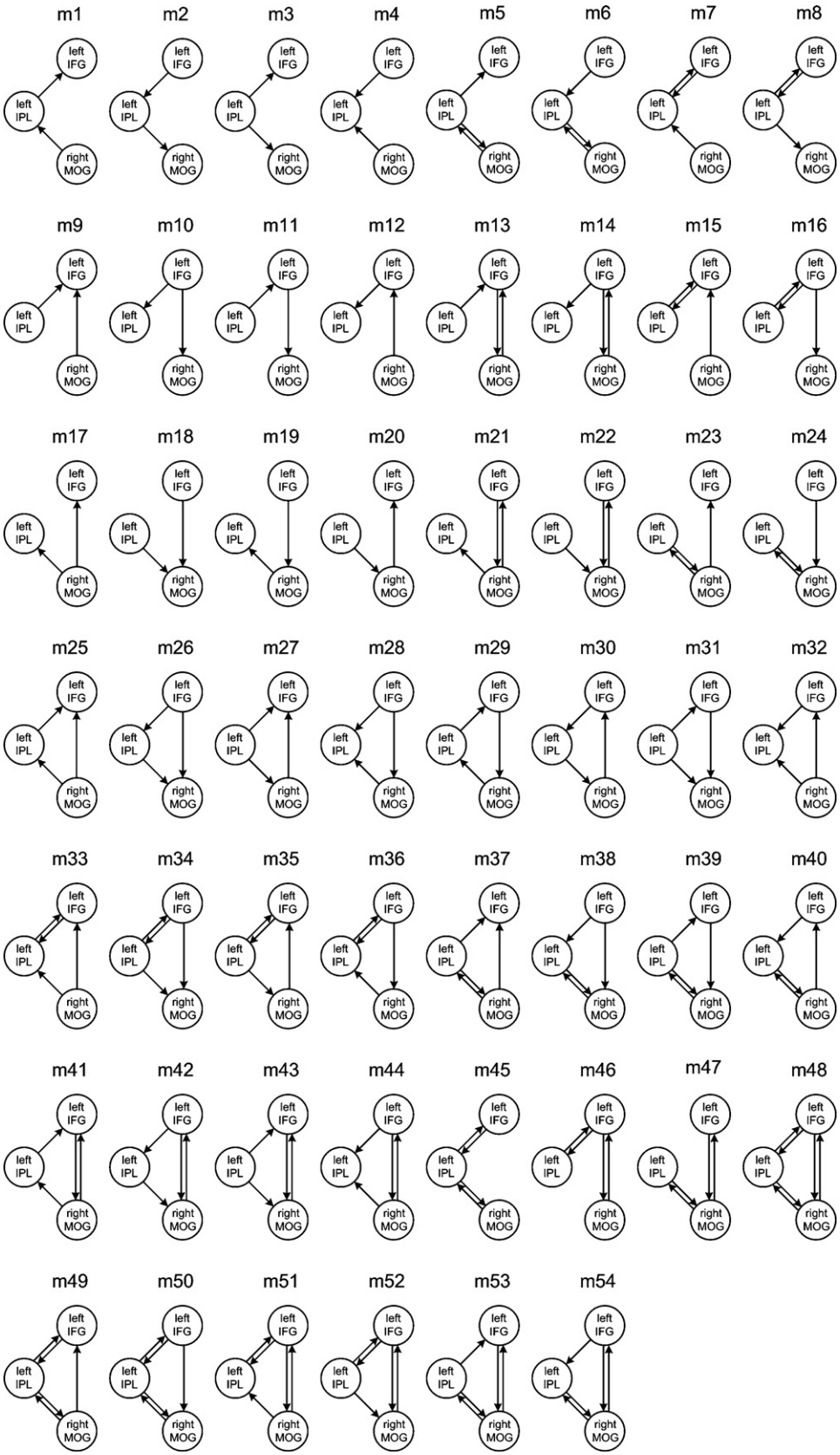

Fig. 3. Model 1–Model 54. For each candidate model, the arrowed line between two regions indicates a directional modulatory effect of letter-response specified at the intrinsic connection between those two regions. MOG, the middle occipital gyrus; IPL, the inferior parietal lobules; IFG, the inferior frontal gyrus.

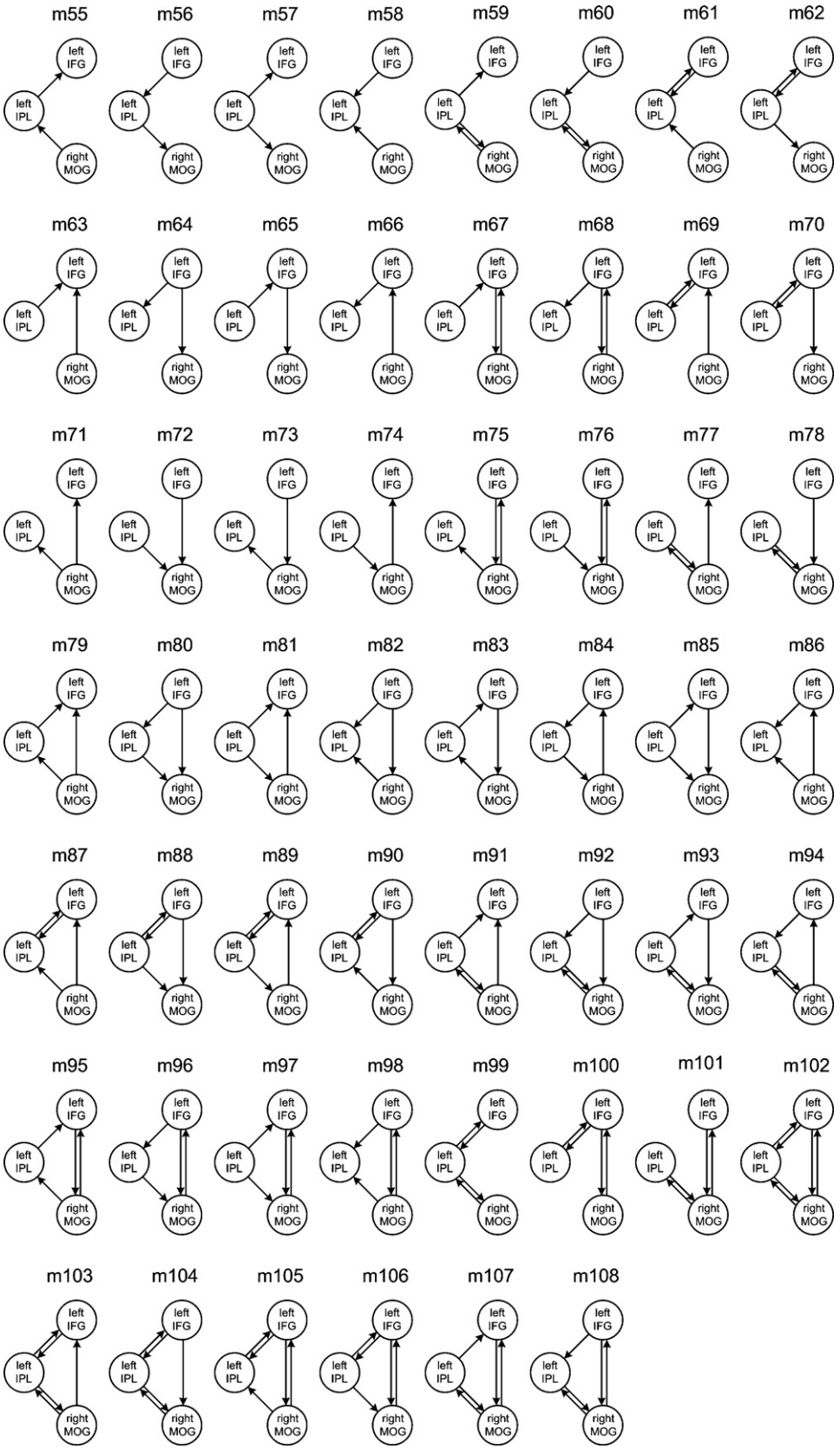

Fig. 4. Model 55–Model 108. For each candidate model, the arrowed line between two regions indicates a directional modulatory effect of letter response as well as a directional modulatory effect of no-letter response specified at the intrinsic connection between those two regions. MOG, the middle occipital gyrus; IPL, the inferior parietal lobules; IFG, the inferior frontal gyrus.

Table 2
Individual VOI corresponding to each activated region of letter response relative to no-letter response.

	Left IFG			Left IPL			Right MOG		
	x	*y*	*z*	*x*	*y*	*z*	*x*	*y*	*z*
Participant01	−46	−2	34	−40	−40	42	48	−52	−8
Participant02	−52	12	24	−38	−48	42	52	−54	−10
Participant03	−50	8	36	−38	−58	54	50	−64	−14
Participant04	−44	6	20	−36	−46	48	50	−54	−16
Participant05	−50	4	30	−38	−44	52	46	−54	−8
Participant06	−40	8	24	−32	−58	48	46	−66	−10
Participant07	−52	8	28	−34	−46	46	48	−60	−14
Participant08	−50	6	36	−42	−52	54	44	−64	−10
Participant09	−54	8	36	−40	−48	58	50	−60	−16
Participant10	−58	6	28	−34	−42	44	42	−62	−18
Participant11	−52	4	32	−32	−40	46	52	−62	−4
Participant12	−48	8	28	−42	−40	48	48	−54	−16
Participant13	−58	6	28	−36	−48	56	48	−52	−14
Participant14	−56	16	30	−34	−42	58	52	−60	−8
Participant15	−54	8	34	−44	−42	46	46	−60	−12
Participant16	−54	8	28	−44	−50	50	48	−60	−14
Participant17	−52	0	34	−46	−38	60	56	−62	−14
Mean	−51	7	30	−38	−46	50	49	−59	−12
Std	5	4	5	4	6	6	3	5	4

The loci of VOIs are labeled using MNI coordinate. IFG, inferior frontal gyrus; IPL, inferior parietal lobule; MOG, middle occipital gyrus.

corrected) and a cluster threshold $k > 30$, while the reverse comparison did not identify significant activations anywhere in the brain (Table 1).

For the functional localizer session using the same significance and cluster thresholds as the above, regions showing more activation for passively viewed real letters compared to pure noise images were identified within the right fusiform gyrus (Table 1 and Fig. 2B).

3.2. DCM results

Supplemental Table 1 reports the GBF for each pairwise Bayesian model selection between the candidate models averaged across the 17 subjects. Supplemental Tables 2 and 3 report the frequency across 17 participants that each model was the most likely as a result of the pairwise Bayesian model selection with the criteria of BF > 3 (PER) and BF > 1, respectively. As revealed by these results, Model 19 (M19) was superior to the other candidate models at the group level (i.e., across the 17 participants). For the convenience of description, Table 3 summarizes the results of Bayesian model selection between the best model (i.e., M19) and the other candidate models. Fig. 5 shows the intrinsic connections and the modulatory effects induced by letter responses for M19.

When viewing pure noise images in general (i.e., the intrinsic connections), the right MOG, the left IPL, and the left IFG were reciprocally connected ($ps < 0.002$). In contrast, regarding the modulatory effect, when a letter was falsely detected while viewing a pure noise image, the feed-backward connection from the left IFG to the right MOG ($t(16) = 3.285$, $p = 0.005$) and the feed-forward connection from the right MOG to the left IPL ($t(16) = 12.856$, $p < 0.001$) were both significantly enhanced.

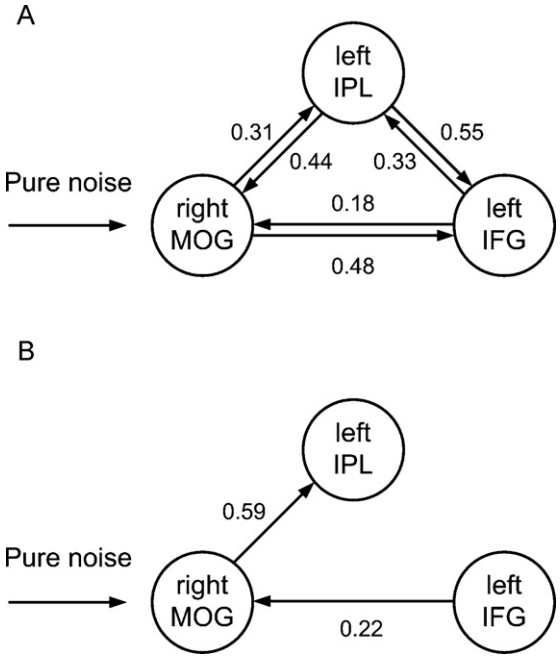

Fig. 5. Results from the best model (M19) selected by Bayesian model selection. (A) The intrinsic connections of M19. With a pure noise image as input, the right MOG, the left IPL and the left IFG were reciprocally connected to each other ($ps < 0.002$). (B) The modulatory effect of detecting a letter when viewing a pure noise image. When the participant detected a letter, both the feed-forward connection from the right MOG to the left IPL ($t(16) = 12.856$, $p < 0.001$) and the feed-backward connection from the left IFG to the right MOG ($t(16) = 3.285$, $p = 0.005$) were enhanced. MOG, the middle occipital gyrus; IPL, the inferior parietal lobules; IFG, the inferior frontal gyrus.

4. Discussion

We used DCM to investigate the effective functional connectivity between regions of the cortical network that underlie top-down letter processing. As indicated by the optimal model (i.e., M19), when a letter was 'detected' while viewing a pure noise image, the feed-backward connection from the left IFG to the right MOG and the feed-forward connection from the right MOG to the left IPL were both enhanced.

One may argue that such modulatory effect was possibly due to the shared effect of the letter response and no-letter responses (e.g., viewing pure noise images or task demand itself) rather than the illusory letter detection *per se*. However, M19 only included the modulatory effect of the letter responses and was found to be superior to all other candidate models, especially including the models with the modulatory effects of both the letter responses and no-letter responses. Thus, the significant modulatory effects found in the present DCM analysis were likely to be generated by participants' illusory detection of letters.

Recent studies suggest that object specific expectations are implemented within the brain via an internal template (Beck & Kastner, 2009; Summerfield et al., 2006). When we look for a spe-

Table 3
The results of Bayesian model selection between M19 and the other candidate models.

Models	GBF	>3	>1	Models	GBF	>3	>1	Models	GBF	>3	>1
M1	3.9E+06	(7,1)	(11,6)	M37	1.2E+19	(14,0)	(15,1)	M73	4.2E+13	(13,0)	(14,1)
M2	7.2E+67	(11,2)	(14,3)	M38	1.9E+13	(13,0)	(15,0)	M74	6.3E+20	(13,2)	(14,3)
M3	2.0E+80	(12,1)	(14,3)	M39	3.1E+14	(15,1)	(16,1)	M75	5.9E+20	(13,0)	(13,0)
M4	2.3E+07	(6,0)	(12,5)	M40	1.1E+16	(14,0)	(16,1)	M76	3.6E+29	(14,0)	(14,0)
M5	2.9E+11	(11,1)	(16,1)	M41	2.8E+13	(13,1)	(14,2)	M77	3.3E+22	(13,0)	(14,0)
M6	4.2E+09	(10,1)	(15,1)	M42	5.2E+23	(15,1)	(15,1)	M78	3.2E+28	(14,0)	(15,0)
M7	2.0E+13	(14,1)	(16,1)	M43	4.8E+19	(15,1)	(15,1)	M79	2.3E+23	(13,1)	(14,1)
M8	5.6E+76	(13,1)	(15,1)	M44	6.6E+13	(13,1)	(14,2)	M80	1.8E+74	(16,0)	(16,0)
M9	1.1E+15	(10,3)	(12,5)	M45	3.5E+19	(15,1)	(16,1)	M81	1.4E+28	(13,1)	(13,1)
M10	1.1E+75	(11,2)	(14,3)	M46	3.4E+22	(15,0)	(15,1)	M82	1.4E+15	(11,0)	(14,1)
M11	3.2E+76	(10,2)	(12,5)	M47	2.4E+11	(13,2)	(14,2)	M83	1.5E+10	(13,2)	(13,2)
M12	8.1E+16	(10,2)	(14,3)	M48	1.2E+27	(15,0)	(15,0)	M84	1.6E+29	(14,1)	(14,1)
M13	6.5E+14	(12,1)	(15,1)	M49	1.2E+24	(15,0)	(16,0)	M85	9.2E+82	(15,0)	(16,0)
M14	2.1E+19	(13,1)	(15,1)	M50	6.1E+22	(16,0)	(16,0)	M86	3.1E+18	(11,1)	(13,1)
M15	4.1E+21	(14,1)	(15,1)	M51	6.3E+21	(14,0)	(14,0)	M87	7.9E+26	(13,0)	(13,1)
M16	1.8E+77	(12,1)	(14,1)	M52	3.3E+27	(15,0)	(16,0)	M88	5.4E+86	(16,0)	(16,0)
M17	7.9E+17	(8,4)	(11,6)	M53	1.3E+20	(14,0)	(15,1)	M89	8.4E+36	(13,0)	(13,0)
M18	2.4E+75	(11,2)	(13,4)	M54	1.3E+20	(14,0)	(15,0)	M90	2.7E+16	(12,1)	(12,1)
M19	0.0E+00	(0,0)	(0,0)	M55	1.2E+17	(8,2)	(13,3)	M91	7.6E+28	(13,0)	(13,0)
M20	1.3E+09	(9,3)	(11,6)	M56	6.0E+59	(13,0)	(16,1)	M92	1.7E+25	(13,0)	(13,0)
M21	2.4E+04	(9,2)	(12,3)	M57	4.1E+76	(13,0)	(15,1)	M93	4.8E+20	(14,1)	(14,1)
M22	4.1E+12	(10,1)	(15,1)	M58	1.5E+11	(8,2)	(11,2)	M94	9.3E+26	(13,0)	(14,0)
M23	1.8E+14	(11,1)	(13,1)	M59	5.7E+21	(14,1)	(14,1)	M95	1.2E+27	(13,0)	(13,0)
M24	1.1E+06	(6,1)	(14,1)	M60	6.0E+13	(10,0)	(13,0)	M96	2.7E+39	(14,0)	(14,0)
M25	3.6E+17	(10,1)	(12,2)	M61	6.8E+10	(11,2)	(12,2)	M97	2.3E+33	(13,0)	(14,0)
M26	1.4E+71	(13,1)	(13,1)	M62	8.3E+72	(15,0)	(16,0)	M98	1.7E+26	(13,0)	(13,0)
M27	1.4E+18	(12,1)	(15,1)	M63	8.2E+20	(11,2)	(12,3)	M99	3.0E+24	(13,0)	(13,0)
M28	4.7E+08	(10,0)	(16,0)	M64	5.7E+67	(15,0)	(16,0)	M100	1.0E+36	(12,0)	(13,0)
M29	9.8E+06	(12,1)	(16,1)	M65	3.0E+75	(12,0)	(15,1)	M101	8.7E+30	(13,0)	(13,0)
M30	2.3E+17	(14,1)	(15,1)	M66	1.2E+24	(13,2)	(13,3)	M102	1.7E+43	(13,0)	(15,0)
M31	4.8E+78	(12,1)	(15,1)	M67	2.3E+25	(13,1)	(13,1)	M103	7.1E+33	(12,0)	(14,0)
M32	9.0E+12	(10,1)	(13,1)	M68	1.4E+36	(14,0)	(14,1)	M104	7.8E+22	(12,1)	(14,1)
M33	1.8E+24	(14,0)	(15,0)	M69	1.8E+28	(11,2)	(13,2)	M105	8.6E+32	(12,0)	(13,0)
M34	1.2E+79	(13,1)	(15,1)	M70	1.9E+79	(15,0)	(15,0)	M106	1.7E+44	(13,0)	(13,0)
M35	1.5E+23	(15,1)	(15,1)	M71	8.9E+16	(11,3)	(12,3)	M107	2.1E+37	(13,0)	(13,0)
M36	8.1E+15	(16,1)	(16,1)	M72	1.7E+70	(14,1)	(15,1)	M108	1.0E+36	(13,0)	(14,0)

The left numbers in the brackets of column labeled by ">3" and ">1" indicate the frequency across 17 participants that the M19 won the other corresponding models with criterion of BF > 3 and BF > 1, respectively, while the right numbers indicate the results of the reverse comparisons. GBF, group Bayes factor.

cific object in the environment, we attempt to match the bottom-up information against its internal template. Bottom-up visual features that match are weighted more heavily, which biases our perception in favor of the expected object (Beck & Kastner, 2009). In the present study, participants were trained with real letters before viewing pure noise images. Perhaps this training served to prime letter specific expectations such that participants readily reported seeing letters among the pure noise images when certain features of these pure noise images appeared to resemble those of letters.

As revealed by our DCM analysis, when a letter was 'detected' while viewing a pure noise image, the response of the right MOG was enhanced via increased connectivity from the left IFG. The locus of the right MOG (Fig. 2A, red circle, Talairach: 51, −59, −7) was consistent with that found in the recent studies such as Pernet, Celsis, and Demonet (2005) (Talairach: 46, −63, −12) and Gauthier et al. (2000) (Talairach: 50, −59, 3). It was also consistent with the cortical regions (Fig. 2B, green circle, Talairach: 48, −55, −6) identified through our functional localizer task that compared easily seen real letters to pure noise images. Our results indicate that the response of the letter-preferential regions in the visual cortex can be modulated by top-down influences from the prefrontal cortex.

Recent studies (for a review see Beck & Kastner, 2009; Miller & D'Esposito, 2005) support our finding that there is a feed-backward connection from the left prefrontal cortex to the occipitotemporal cortex. For example, Mechelli et al. (2004) found that when participants imagined objects from a particular category (e.g., faces, house, and chairs), the responses of category-preferential regions within the occipitotemporal cortex preferentially associated with that category were enhanced by increased connectivity from the left prefrontal cortex to these regions. Additionally, studies of illusory face detection with the same paradigm used in the current study found that the left IFG (Talairach: −48, 13, 24) and the face-preferential region of the occipitotemporal cortex (i.e., the Fusiform Face Area, FFA; Kanwisher & Yovel, 2006) were both activated by face responses relative to no-face responses (Zhang et al., 2008). Moreover, the functional connectivity between these two regions was greater for face responses than for no-face responses (Talairach: −50, 3, 24, Li et al., 2009).

Our results provide additional evidence in support of the claim that category-preferential regions within the visual cortex are modulated by top-down signals originating in higher cortical regions such as the prefrontal cortex (Heekeren, Marrett, Bandettini, & Ungerleider, 2004; Kastner & Ungerleider, 2000; Miller & D'Esposito, 2005). In the present study, the left IFG was more active when the participant 'detected' a letter when viewing a pure noise image. Increased activation of the left IFG has also been reported in other top-down word and letter processing related tasks (e.g., object naming [Talairach: −47, 5, 27, Joseph et al., 2006], imagined letters [Talairach: −43, 15, 23, James & Gauthier, 2006], and word generation [MNI: −45, 4, 35, Tremblay & Gracco, 2006]), as well as non-word processing tasks (e.g., illusory face detection [Talairach: −53, 7, 29, Li et al., 2010] and perception of impoverished objects [Talairach: −40, 5, 25, Ganis, Schendan, & Kosslyn, 2007]). The loci of activation in these studies were consistent with the region identified in the present study (Talairach: −51, 7, 27). Additionally, James and Gauthier (2006) found that this region is activated by writing the first letter of the word that names a presented shape as compared to drawing that shape. This finding

suggests that the left IFG also plays a significant role in retrieving letter shapes from memory. Note that the cognitive operations in all above-mentioned studies require the access of our existing knowledge about the properties or meanings of certain objects. Thus, the left IFG may be involved in the successful retrieval of semantic information from memory, which can facilitate the subsequent top-down processing (Curtis & D'Esposito, 2003; Ganis et al., 2007). Our DCM results, taken together with these existing findings, suggest that the left IFG may provide an important top-down signal based on the expected (e.g., remembered) letter shapes. On this account, the left IFG sends a top-down signal to the visual cortex (i.e., the right MOG) to search for letter features in the visual input, which in turn biases participants to falsely detect letters when viewing pure noise images by highlighting letter-like features contained within the noise images (Gilbert & Sigman, 2007; Miller & D'Esposito, 2005).

Our DCM results also revealed increased connectivity from the right MOG to the left IPL when letters were "detected". In the present study, the left IPL, like the left IFG, was more active when letters were 'detected' when viewing a pure noise image. In line with our results, recent studies found that the left IPL is more involved in letter naming than letter discrimination, which suggest that this region may be selectively involved in the phonological translation of letters into sounds (Joseph et al., 2006). Furthermore, the locus of the left IPL in these studies (−38, −50, 48) was consistent with the present finding (−40, −44, 50). The suggestion that the left IPL plays a role in phonological decoding is also supported by converging evidence from other neuroimaging (Price, Wise, & Frackowiak, 1996) and neuropsychological (Friedman, Ween, & Albert, 1993) studies. Unlike faces, which are a highly similar class of object, each letter has a distinct shape and a distinct sound. These two modalities of letter perception are so interconnected that when a letter is identified based on one modality (e.g., shape), the other modality (e.g., phonology) is automatically evoked. Demonstrating this connection in the current study, many participants reported silently reading the letter they 'found' in the pure noise images even though their only task was simple letter detection by means of a button press rather than letter identification. On this account, when the bottom-up information of a pure noise image contained features suggestive of a particular letter, the right MOG may have provided the identity of that letter to the left IPL whereupon that letter was mapped into the corresponding phonological information. Thus, the increased connectivity from the right MOG to the left IPL on letter detection trials may have supported retrieval of phonological information for the specific illusory letter that was detected.

One caveat should be noted about the present findings. The present study used a relatively rapid event-related design, for an important reason. As indicated by the behavior results of the present study, the illusory detection of letters from noise-only images was relatively rare (only about 38% with a SD of 20.0%). To increase the statistical power of contrasting trials of the letter responses and those of the no-letter responses for each participant, we needed to include a sufficiently large number of trials. However, the task was relatively difficult and demanded a greatly enhanced level of attention, a prolonged scanning time would likely have produced inattention, fatigue, or other possible confounds. The present design thus attempted to strike a balance in meeting these two constraints. However, the reduced inter-stimulus interval (ISI) might have reduced experimental efficiency because the hemodynamic responses elicited in different conditions were largely overlapped. In future studies, one could improve the experimental efficiency by both increasing and varying the ISI, the implementation of which may require data collection in multiple sessions.

5. Conclusion

In the present study, we investigate the neural interactions between regions of the cortical network involved in top-down letter processing. When participants 'detected' letters when viewing pure noise images, the response of a letter-preferential region within the visual cortex (i.e., the right MOG) was enhanced by the increased connectivity from the left IFG. The response of the left IPL was in turn enhanced by increased connectivity from the right MOG. Our results suggest that the top-down signal for letter processing originates in the left IFG, which directly affects the visual cortex. This feed-backward connection may facilitate the detection of letters by increasing the activity of the cortical region that represents the features contained within each letter. In turn, the specific letter identity is forwarded to the left IPL by means of increased connectivity, which may facilitate retrieval of the phonological information associated with that letter. Our findings also suggest that letter processing and perhaps the processing of many other visual stimuli (e.g., faces) may involve active interactions between top-down signals from the prefrontal cortex and bottom-up information from the visual cortex.

Acknowledgements

This paper is supported by the Knowledge Innovation Project of the Chinese Academy of Sciences under Grant No. KGCX2-YW-129, the National Natural Science Foundation of China under Grant No. 30970771, 30873462, 60910006, 30970769, 31028010, 81000640, the Project for the National Basic Research Program of China (973) under Grant No. 2006CB705700, Program for Changjiang Scholars and Innovative Research Team in University (PCSIRT) under Grant No. IRT0645, NSERC, and NIH (R01HD046526 and R01HD060595).

Appendix A. Supplementary data

Supplementary data associated with this article can be found, in the online version, at doi:10.1016/j.neuropsychologia.2011.01.011.

References

Beck, D. M., & Kastner, S. (2009). Top-down and bottom-up mechanisms in biasing competition in the human brain. *Vision Research*, *49*, 1154–1165.
Bitan, T., Booth, J. R., Choy, J., Burman, D. D., Gitelman, D. R., & Mesulam, M. M. (2005). Shifts of effective connectivity within a language network during rhyming and spelling. *The Journal of Neuroscience*, *25*, 5397–5403.
Chow, H. M., Kaup, B., Raabe, M., & Greenlee, M. W. (2008). Evidence of fronto-temporal interactions for strategic inference processes during language comprehension. *NeuroImage*, *40*, 940–954.
Cohen, L., & Dehaene, S. (2004). Specialization within the ventral stream: The case for the visual word form area. *NeuroImage*, *22*, 466–476.
Cohen, L., Martinaud, O., Lemer, C., Lehericy, S., Samson, Y., Obadia, M., Slachevsky, A., & Dehaene, S. (2003). Visual word recognition in the left and right hemisphere: Anatomical and functional correlates of peripheral alexias. *Cerebral Cortex*, *13*, 1313–1333.
Curtis, C. E., & D'Esposito, M. (2003). Persistent activity in the prefrontal cortex during working memory. *Trends in Cognitive Sciences*, *7*, 415–423.
Dehaene, S., Cohen, L., Sigman, M., & Vinckier, F. (2005). The neural code for written words: A proposal. *Trends in Cognitive Sciences*, *9*, 335–341.
Flowers, D. L., Jones, K., Noble, K., VanMeter, J., Zeffiro, T. A., Wood, F. B., & Eden, G. F. (2004). Attention to single letters activates left extrastriate cortex. *NeuroImage*, *21*, 829–839.
Friedman, R. F., Ween, J. E., & Albert, M. L. (1993). Alexia. In K. M. Heilman, & E. Valenstein (Eds.), *Clinical neuropsychology* (3rd ed., pp. 37–62). New York: Oxford University Press.
Friston, K. J., Holmes, A. P., Worsley, K. J., Poline, J. P., Frith, C. D., & Frackowiak, R. S. J. (1995). Statistical parametric maps in functional imaging: A general linear approach. *Human Brain Mapping*, *2*, 189–210.
Friston, K. J., Harrison, L., & Penny, W. (2003). Dynamic causal modeling. *NeuroImage*, *19*, 1273–1302.
Ganis, G., Schendan, H. E., & Kosslyn, S. M. (2007). Neuroimaging evidence for object model verification theory: Role of prefrontal control in visual object categorization. *NeuroImage*, *34*, 384–398.

Gauthier, I., Tarr, M. J., Moylan, J., Skudlarski, P., Gore, J. C., & Anderson, A. W. (2000). The fusiform "face area" is part of a network that processes faces at the individual level. *Journal of Cognitive Neuroscience*, *12*, 495–504.

Gilbert, C. D., & Sigman, M. (2007). Brain states: Top-down influences in sensory processing. *Neuron*, *54*, 677–696.

Heekeren, H. R., Marrett, S., Bandettini, P. A., & Ungerleider, L. G. (2004). A general mechanism for perceptual decision-making in the human brain. *Nature*, *431*, 859–862.

James, K. H., & Gauthier, I. (2006). Letter processing automatically recruits a sensory-motor brain network. *Neuropsychologia*, *44*, 2937–2949.

Joseph, J. E., Gathers, A. D., & Piper, G. A. (2003). Shared and dissociated cortical regions for object and letter processing. *Cognitive Brain Research*, *17*, 56–67.

Joseph, J. E., Cerullo, M. A., Farley, A. B., Steinmetz, N. A., & Mier, C. R. (2006). fMRI correlates of cortical specialization and generalization for letter processing. *NeuroImage*, *32*, 806–820.

Kanwisher, N., & Yovel, G. (2006). The fusiform face area: A cortical region specialized for the perception of faces. *Philosophical Transactions of the Royal Society of London B*, *361*, 2109–2128.

Kastner, S., & Ungerleider, L. G. (2000). Mechanism of visual attention in the human cortex. *Annual Review of Neuroscience*, *23*, 315–341.

Kosslyn, S. M., Alpert, N. M., Thompson, W. L., Maljkovic, V., Weise, S. B., Chabris, C. F., Hamilton, S. E., Rauch, S. L., & Buonanno, F. S. (1993). Visual mental imagery activates topographically organized visual cortex: PET investigations. *Journal of Cognitive Neuroscience*, *5*, 263–287.

Li, J., Liu, J., Liang, J., Zhang, H., Zhao, J., Huber, D. E., Rieth, C. A., Lee, K., Tian, J., & Shi, G. (2009). A distributed neural system for top-down face processing. *Neuroscience Letters*, *451*, 6–10.

Li, J., Liu, J., Liang, J., Zhang, H., Zhao, J., Rieth, C. A., Huber, D. E., Li, W., Shi, G., Ai, L., Tian, J., & Lee, K. (2010). Effective connectivities of cortical regions for top-down face processing: A dynamic causal modeling study. *Brain Research*, *1340*, 40–51.

Liu, J., Li, J., Zhang, H., Rieth, C. A., Huber, D. E., Li, W., Lee, K., & Tian, J. (2010). Neural correlates of top-down letter processing. *Neuropsychologia*, *48*, 636–641.

McCandliss, B. D., Cohen, L., & Dehaene, S. (2003). The visual word form area: Expertise for reading in the fusiform gyrus. *Trends in Cognitive Sciences*, *7*, 293–299.

Mechelli, A., Price, C. J., Friston, K. J., & Ishai, A. (2004). Where bottom-up meets top-down: Neuronal interactions during perception and imagery. *Cerebral Cortex*, *14*, 1256–1265.

Miller, B. T., & D'Esposito, M. (2005). Searching for "the top" in top-down control. *Neuron*, *48*, 535–538.

Nazir, T. A., Jacobs, A. M., & O'Regan, J. K. (1998). Letter legibility and visual word recognition. *Memory & Cognition*, *26*, 810–821.

Pelli, D. G., Farell, B., & Moore, D. C. (2003). The remarkable inefficiency of word recognition. *Nature*, *423*, 752–756.

Penny, W. D., Stephan, K. E., Mechelli, A., & Friston, K. J. (2004). Comparing dynamic causal models. *NeuroImage*, *22*, 1157–1172.

Pernet, C., Celsis, P., & Demonet, J.-F. (2005). Selective response to letter categorization within the left fusiform gyrus. *NeuroImage*, *28*, 738–744.

Price, C. J., & Devlin, J. T. (2003). The myth of the visual word form area. *NeuroImage*, *19*, 473–481.

Price, C. J., Wise, R. J., & Frackowiak, R. S. (1996). Demonstrating the implicit processing of visually presented words and pseudowords. *Cerebral Cortex*, *6*, 62–70.

Raftery, A. E. (1995). Bayesian model selection in social research. In P. V. Marsden (Ed.), *Sociological methodology* (pp. 111–163). Cambridge, MA: Blackwell.

Reicher, G. M. (1969). Perceptual recognition as a function of meaningfulness of stimulus material. *Journal of Experimental Psychology*, *81*, 275–280.

Reinke, K., Fernandes, M., Schwindt, G., O'Craven, K., & Grady, C. L. (2008). Functional specificity of the visual word form area: General activation for words and symbols but specific network activation for words. *Brain and Language*, *104*, 180–189.

Stephan, K. E., & Penny, W. D. (2006). Dynamic causal models and Bayesian selection. In K. J. Friston (Ed.), *Statistical parametric mapping: The analysis of functional brain images* (pp. 577–585). Amsterdam: Elsevier.

Stephan, K. E., Marshall, J. C., Penny, W. D., Friston, K. J., & Fink, G. R. (2007). Interhemispheric integration of visual processing during task-driven lateralization. *The Journal of Neuroscience*, *27*, 3512–3522.

Stephan, K. E., Penny, W. D., Daunizeau, J., Moran, R. J., & Friston, K. J. (2009). Bayesian model selection for group studies. *NeuroImage*, *46*, 1004–1017.

Stephan, K. E., Penny, W. D., Moran, R. J., den Ouden, H. E. M., Daunizeau, J., & Friston, K. J. (2010). Ten simple rules for dynamic causal modeling. *NeuroImage*, *49*, 3099–3109.

Stokes, M., Thompson, R., Cusack, R., & Duncan, J. (2009). Top-down activation of shape-specific population codes in visual cortex during mental imagery. *The Journal of Neuroscience*, *29*, 1565–1572.

Summerfield, C., Egner, T., Greene, M., Koechlin, E., Mangels, J., & Hirsch, J. (2006). Predictive codes for forthcoming perception in the frontal cortex. *Science*, *314*, 1311–1314.

Tremblay, P., & Gracco, V. L. (2006). Contribution of the frontal lobe to externally and internally specified verbal responses: fMRI evidence. *NeuroImage*, *33*, 947–957.

Vinckier, F., Dehaene, S., Jobert, A., Dubus, J. P., Sigman, M., & Cohen, L. (2007). Hierarchical coding of letter strings in the ventral stream: Dissecting the inner organization of the visual word-form system. *Neuron*, *55*, 143–156.

Zhang, H., Liu, J., Huber, D. E., Rieth, C. A., Tian, J., & Lee, K. (2008). Detecting faces in pure noise images: A functional MRI study on top-down perception. *NeuroReport*, *19*, 229–233.